Microbial Cell Factories

RESEARCH Open Access

Engineering serine metabolism to enhance *AOX1* promoter self-induction in formate dehydrogenase-deficient *Komagataella phaffii*

Rocio Cozmar[1,2], Julio Berrios[2] and Patrick Fickers[1*]

Abstract

Background The methylotrophic yeast *Komagataella phaffii* is a premier host for recombinant protein (rProt) production, which traditionally relies on methanol induction of the alcohol oxidase 1 promoter (P_{AOX1}). However, the flammability and associated industrial limitations of methanol have motivated the search for methanol-free induction systems. We recently demonstrated that disruption of formate dehydrogenase gene (FDH) in *K. phaffii* allows endogenous formate derived from tetrahydrofolate (THF)-mediated C1 metabolism to induce P_{AOX1} without the addition of external inducers. Therefore, we hypothesized that increasing intracellular formate production by enhancing serine biosynthesis could further improve promoter induction and rProt productivity.

Results Overexpression of *SER3*, encoding 3-phosphoglycerate dehydrogenase, the rate-limiting enzyme in serine synthesis, significantly increased P_{AOX1}-driven expression of an intracellular reporter protein (eGFP) and secreted glucose oxidase (Gox) from *Aspergillus niger* without compromising cell fitness. Enhanced formate accumulation and stronger P_{AOX1} induction were observed in both microbioreactor and bioreactor cultivations using sorbitol or glycerol-sorbitol mixtures. In GOX-*m*SER3 strain grown in bioreactor, *SER3* overexpression led to a 30% increase in specific Gox activity compared with that of the parental FdhKO strain.

Conclusions This study provides a cost-effective metabolic engineering strategy for methanol-free, self-inducible expression systems in *K. phaffii* based on P_{AOX1}, enabling safer and more sustainable industrial rProt production.

Keywords *Komagataella phaffii*, Formate, Formate dehydrogenase, Serine metabolism, *AOX1* promoter, Recombinant protein

*Correspondence:
Patrick Fickers
pfickers@Uliege.be
[1]Microbial Processes and Interactions, TERRA Teaching and Research Centre, Gembloux Agro-Bio Tech, University of Liege, Gembloux, Belgium
[2]School of Biochemical Engineering, Pontificia Universidad Católica de Valparaíso, Valparaiso, Chile

Background

The methylotrophic yeast *Komagataella phaffii* (formerly *Pichia pastoris* [1]), is widely used as a host for recombinant protein (rProt) production [2]. In addition to expression systems based on constitutive promoters, among other P_{GAP}, P_{TEF}, or P_{UPP}, that drive continuous rProt synthesis [3, 4], many bioprocesses rely on strategies that decouple cell growth from the rProt production phase. This approach mitigates the cellular burden associated with rProt synthesis and secretion during biomass formation, thereby improving overall process performance.

Historically, the tightly regulated promoter of the alcohol oxidase 1 gene (P_{AOX1}) has been predominantly employed. This promoter is repressed in the presence of glucose or glycerol, derepressed upon their depletion, and robustly induced by methanol [5]. However, the industrial use of methanol presents several challenges, including flammability, high oxygen demand during methanol catabolism, and stringent safety and regulatory requirements [6, 7].

To address these limitations, several approaches have been explored, including the development of mutated P_{AOX1} variants [8] substrate co-feeding strategies [9, 10] or the modification of the P_{AOX1} regulation through core promoter engineering or co-expression of transcription factors [11, 12]. More recently, so-called derepressed promoters have emerged as promising alternatives to methanol-dependent systems. In such systems, gene expression is triggered upon depletion of the primary carbon source or under carbon-limited conditions. For instance, the P_{DH} promoter and variants derived from the heat shock gene *HSP12* are strongly induced under carbon starvation and have been investigated as next-generation promoters enabling inducer-free, growth-decoupled regulation [13, 14]. Another line of research has focused on identifying alternative inducers for P_{AOX1} that provide a safer and more manageable substitute for methanol. Formate, an intermediate of the methanol catabolism, has been evaluated as a putative P_{AOX1} inducer in strains exhibiting different methanol utilization phenotypes (Mut^+, Mut^S, and Mut^-) [15–18]. However, across all phenotypes, formate concentrations above 20 mM were shown to negatively affect the specific growth rate, indicating potential cytotoxic effects [16]. As a C1 molecule with a low energy content, formate must be supplemented with a non-repressive carbon source during the rProt production phase. Sorbitol has proven to be an effective co-substrate in this context [9, 16, 19]. Metabolically, formate is an intermediate in the methanol dissimilative pathway, where it is oxidized to carbon dioxide by formate dehydrogenase (Fdh) [12]. Additionally, formate is a key intermediate in tetrahydrofolate-mediated one-carbon (THF-C1) metabolism, which contributes to several anabolic processes, including de novo purine synthesis [20] (Additional File 1: Figure S1). The THF-C1 pathway operates in both the mitochondria and the cytoplasm, with formate serving as a C1 shuttle between the two compartments.

Recently, we demonstrated that *K. phaffii* cells lacking formate dehydrogenase (FdhKO) specifically generate formate through the THF–C1 pathway and that this endogenous formate is capable of inducing P_{AOX1} [21]. When cultivated in sorbitol-based medium, the FdhKO mutant partially exported formate into the culture supernatant, likely via carboxylate transporters [22], leading to extracellular concentrations of up to 15 µM (0.7 $mg{\cdot}L^{-1}$). By contrast formate was not detected for the non-disrupted strain. The FdhKO mutant and the non-disrupted strain exhibited comparable growth kinetics on sorbitol, indicating that formate accumulation was not toxic under these conditions. Notably, the endogenous formate produced by the FdhKO strain induced P_{AOX1} to levels comparable to those obtained with methanol induction [21]. This was demonstrated using the secreted model protein lipase CalB, for which the maximal specific activities were similar on sorbitol and sorbitol–methanol media (136 and 113 $U{\cdot}mgDCW^{-1}$, respectively; [21]. Formate accumulation and P_{AOX1} induction were further modulated by strain genotype and culture conditions. Enhancing sorbitol uptake in the FdhKO eGFP strain (fdh1Δ, P_{AOX1}-eGFP) through constitutive expression of sorbitol dehydrogenase increased the specific growth rate from 0.036 h^{-1} to 0.119 h^{-1}, while markedly reducing eGFP fluorescence and consequently P_{AOX1} induction. Likewise, cultivation of the FdhKO eGFP strain under different oxygen transfer conditions (OTC, k_La values of 10, 50, and 100 h^{-1} representing low, medium and high OTC, respectively) resulted in significantly higher formate accumulation and eGFP expression at k_La values of 10 and 50 h^{-1}. In contrast, the growth rate remained unchanged across all OTCs (average value of 0.039 h^{-1}), indicating that oxygen availability did not limit cell growth under these conditions [23]. Furthermore, when the FdhKO mutant was cultivated on a glycerol–sorbitol mixture, P_{AOX1} induction occurred only after glycerol depletion and reached levels significantly higher than those observed during simple de-repression on glycerol medium [23]. Collectively, these findings demonstrate that disruption of the Fdh-encoding gene enables *K. phaffii* to autonomously generate formate, resulting in P_{AOX1} self-induction. This provides a novel strategy for converting any P_{AOX1}-based expression system into a fully self-inducing platform in an FdhKO background.

In THF-C1 metabolism, formate is derived from serine. We previously showed that serine supplementation markedly increases P_{AOX1} induction and rProt productivity [21]. Serine is synthesized from the glycolytic intermediate 3-phosphoglycerate through three enzymatic steps

involving phosphoglycerate dehydrogenase (Pgdh), phosphoserine aminotransferase (PSat1), and phosphoserine phosphatase (Psph), encoded by *SER3*, *SER1*, and *SER2*, respectively [24, 25] (Fig. 1). In *Saccharomyces cerevisiae*, this pathway is tightly regulated, as serine represses *SER1* transcription [26], whereas *SER3* expression is modulated by the noncoding RNAi *SRG1* [24, 27]. In addition, serine can be reversibly converted from glycine by serine hydroxymethyltransferases Shm1 and Shm2, which also participate in THF-C1 metabolism [28] (Additional File 1: Figure S1).

Given that serine supplementation is not economically viable at an industrial scale, we further engineered the FdhKO strain by overexpressing the SER genes individually or in combination. This strategy was designed to increase intracellular formate accumulation and thereby strengthen P_{AOX1} driven gene expression under methanol-free conditions. Specifically, the overexpression of *SER3* led to increased formate accumulation and, consequently, stronger P_{AOX1} induction. This effect was exemplified herein by a 30% increase in the specific activity of secreted glucose oxidase (Gox) from *Aspergillus niger*, which was used here as a model heterologous rProt.

Results and discussion

Overexpression of the 3-phosphoglycerate dehydrogenase-encoding gene in a FdhKO strain increases formate accumulation and P_{AOX1} induction

Serine is a metabolic precursor in various anabolic pathways and serves as a donor of one-carbon units in the THF-C1 pathway, where formate is a key metabolite. We previously demonstrated that endogenous formate induces the P_{AOX1} promoter in an FdhKO strain and that supplementing the culture medium with serine positively influences P_{AOX1} induction and, consequently, rProt productivity [21].

We hypothesized that enhancing serine biosynthesis could increase intracellular formate levels in a FdhKO strain and thereby further potentiate P_{AOX1} induction. To test this, genes involved in serine synthesis from 3-phosphoglycerate, namely, *SER1* (Psat1), *SER2* (Psph), and *SER3* (Pgadh) (Additional File 1: Table S1), were overexpressed in an FdhKO strain expressing eGFP under the control of the P_{AOX1} promoter (fdh1Δ, P_{AOX1}-*eGFP*, hereafter referred to as *eGfp* strains for simplicity; Table 1).

Each gene was expressed under the control of constitutive promoters, either the strong P_{GAP} (glyceraldehyde-3-phosphate dehydrogenase) or the weaker P_{MDH3} (malate dehydrogenase 3) [29]. The resulting strains were designated as follows: *g*SER1-eGfp (fdh1Δ, P_{AOX1}-*eGFP*, P_{GAP}-*SER1*), *m*SER1-eGfp (fdh1Δ, P_{AOX1}-*eGFP*, P_{MDH3}-*SER1*), *g*SER2-eGfp (fdh1Δ, P_{AOX1}-*eGFP*, P_{GAP}-*SER2*), *m*SER2-eGfp (fdh1Δ, P_{AOX1}-*eGFP*, P_{MDH3}-*SER2*), *g*SER3-eGfp (fdh1Δ, P_{AOX1}-*eGFP*, P_{GAP}-*SER3*), and *m*SER3-eGfp (fdh1Δ, P_{AOX1}-*eGFP*, P_{MDH3}-*SER3*) (Table 1). They were cultivated in microbioreactors in sorbitol medium (YNBS), and specific eGFP fluorescence (i.e., normalized to biomass) was monitored as a proxy to estimate P_{AOX1} induction every 10 min. over 48 h.

For strains overexpressing *SER1* (Psat1) and *SER2* (Psph), no marked difference in cell growth was observed compared with the parental strain (Additional File 1: Figure S2), whereas the specific fluorescence was lower than that of the parental eGFP strain, regardless of the promoter strength used (Fig. 2A, B). In contrast, the overexpression of *SER3*, encoding 3-phosphoglycerate dehydrogenase (Pgadh), resulted in a marked increase in specific fluorescence and consequently P_{AOX1} induction, particularly when it was expressed under the weak P_{MDH3} (1.28-fold vs. 1.18-fold for P_{GAP} after 48 h; Fig. 2C). This strain also presented reduced growth ability, with a 38% lower biomass at 48 h (Additional File 1: Figure S2). Pgadh catalyzes the first reaction of the serine biosynthesis pathway, which has been identified as the rate-limiting step of serine synthesis in *S. cerevisiae* [28]. Based on our

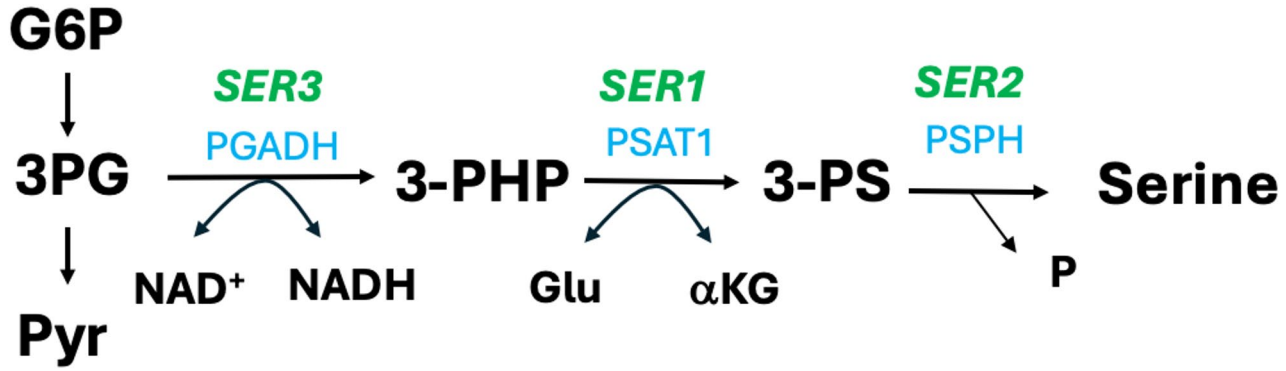

Fig. 1 Serine biosynthesis pathway in *K. phaffii*. PGADH, 3-phophoglycerate dehydrogenase; PSAT1, phosphoserine aminotransferase; PSPH, phosphoserine phosphatase; G6P, glucose-6-phosphate; 3PG, 3-phosphoglycerate; NAD+, nicotinamide adenine dinucleotide oxidized; NADH, nicotinamide adenine dinucleotide reduced; Glu, glutamate; αKG, alfa-ketoglutarate; Pyr, pyruvate; P, phosphate.

Table 1 *K. phaffii* strains used in this study.

Number	Names	Parental strain, relevant genotype	References
RIY232	GS115pro	GS115, HIS4	[30]
RIY230	Fdh eGfp	RIY232, P_{AOX1}-eGFP, Zeo^+	[21]
RIY536	FdhKO eGfp Z^+	RIY230, fdh1Δ, P_{AOX1}-*eGFP*, Zeo^+	[21]
RIY538	FdhKO Z^+	RIY232, fdh1Δ, Zeo^+	This work
RIY539	FdhKO	RIY538, fdh1Δ	This work
RIY540	eGfp	RIY536, fdh1Δ, P_{AOX1}-*eGFP*, Zeo^-	[21]
RIY657	*g*SER1-eGfp	RIY540, fdh1Δ, P_{GAP}-*SER1*, P_{AOX1}-*eGFP*, Zeo^+	This work
RIY658	*m*SER1-eGfp	RIY540, fdh1Δ, P_{MDH3}-*SER1*, P_{AOX1}-*eGFP*, Zeo^+	This work
RIY659	*g*SER2-eGfp	RIY540, fdh1Δ, P_{GAP}-*SER2*, P_{AOX1}-*eGFP*, Zeo^+	This work
RIY660	*m*SER2-eGfp	RIY540, fdh1Δ, P_{MDH3}-*SER2*, P_{AOX1}-*eGFP*, Zeo^+	This work
RIY661	*g*SER3-eGfp	RIY540 fdh1Δ, P_{GAP}-*SER3*, P_{AOX1}-*eGFP*, Zeo^+	This work
RIY662	*m*SER3-eGfp	RIY540, fdh1Δ, P_{MDH3}-*SER3*, P_{AOX1}-*eGFP*, Zeo^+	This work
RIY663	*m*SER3-*g*SER1-eGfp	RIY662, fdh1Δ, P_{MDH3}-*SER3*, P_{GAP}-*SER1*, P_{AOX1}-*eGFP*, Zeo^+, Hyg^+	This work
RIY664	*m*SER3-*m*SER1-eGfp	RIY662, fdh1Δ, P_{MDH3}-*SER3*, P_{MDH3}-*SER1*, P_{AOX1}-*eGFP*, Zeo^+, Hyg^+	This work
RIY655	GOX	RIY539, fdh1Δ, P_{AOX1}-*αMF-GOX*, Zeo^+	This work
RIY665	GOX-SER3	RIY655, fdh1Δ, P_{AOX1}-*αMF-GOX*, P_{MDH3}-*SER3*, Zeo^+, NAT^+	This work

observations, this step is also the rate limiting step for serine anabolism in *K. phaffii*.

As *SER1* expression is downregulated by serine in *K. phaffii* [26], the gene was co-expressed in the *m*SER3-eGfp background (fdh1Δ, P_{AOX1}-*eGFP*, P_{MDH3}-*SER3*) using both the P_{GAP} and P_{MDH3} promoters. The resulting strains, namely, *m*SER3-*g*SER1-eGfp (fdh1Δ, P_{AOX1}-*eGFP*, P_{MDH3}-*SER3*, P_{GAP}-*SER1*) and *m*SER3-*m*SER1-eGfp (fdh1Δ, P_{AOX1}-*eGFP*, P_{MDH3}-*SER3*, P_{MDH3}-*SER1*), were cultivated in microbioreactors under the same experimental conditions (YNBS medium). Compared with that of the parental *m*SER3-eGfp strain, the specific fluorescence signal decreased when *SER1* was expressed under the P_{GAP} promoter (i.e., in the *m*SER3-*g*SER1-eGfp strain), whereas no significant change was observed when P_{MDH3}-driven expression was used (Fig. 2D). The strain overexpressing *SER1* and *SER3* exhibited comparable growth to that of the parental strain, indicating that the expression of these genes does not cause any apparent metabolic imbalance. Taken together, these results suggest that the overexpression of *SER3* exerts a positive indirect effect on P_{AOX1} induction while overexpression of *SER1* in the mSER3–eGFP background does not further enhance P_{AOX1} induction.

In industrial rProt production processes based on P_{AOX1}-driven expression systems, glycerol is commonly used during the cell growth phase, whereas a P_{AOX1} non-repressive carbon source, such as sorbitol, is preferred for the rProt production [9, 30, 31]. Biomass and eGFP fluorescence were therefore monitored for the eGfp (fdh1Δ, P_{AOX1}-*eGFP*) and *m*SER3-eGfp (fdh1Δ, P_{AOX1}-*eGFP*, P_{MDH3}-*SER3*) strains grown in microbioreactors in a mixture of glycerol and sorbitol with ratio 1:2 (YNBGS4). Both strains exhibited diauxic growth, consuming glycerol within the first 8 h of culture followed by a sorbitol consumption phase (Fig. 3A). Both strains grew similarly on both carbon sources, indicating that the overexpression of *SER3* does not affect cell fitness. However, marked differences in specific fluorescence levels and consequently P_{AOX1} induction were observed between the two strains (Fig. 3B). Upon glycerol depletion, eGFP-specific fluorescence markedly increased for both strains. Compared with the eGfp strain, the *SER3* overexpressing strain (i.e., *m*SER3-eGfp) exhibited a 1.5-fold higher specific fluorescence on average between 18 h and 48 h (0.106 vs. 0.072 sFU, respectively). The fluorescence level then tended to decrease slightly as the biomass value reached a plateau (i.e., after 40 h). Although not regulated, the pH of the culture medium only slightly decreased from 6 to 5.7 at the end of the culture (data not shown).

During those cultures, secreted formate in the culture supernatant was monitored over time as a proxy for intracellular accumulation [21, 23]. It increased for both strains after glycerol depletion and peaked at 10 h of culture. Thereafter, the formate concentration gradually decreased for both strains and became nearly undetectable in the culture supernatant by 48 h for the eGFP strain (Fig. 3C). At any time point, the formate content was consistently higher for the *m*SER3-eGFP strain than for the eGFP strain, with the greatest difference observed at 10 h (2-fold, 29 µM vs. 14 µM, respectively). As both strains grew similarly, the accumulation of formate did not affect cell fitness. Furthermore, the formate concentration in the *m*SER3–eGFP strain remained nearly

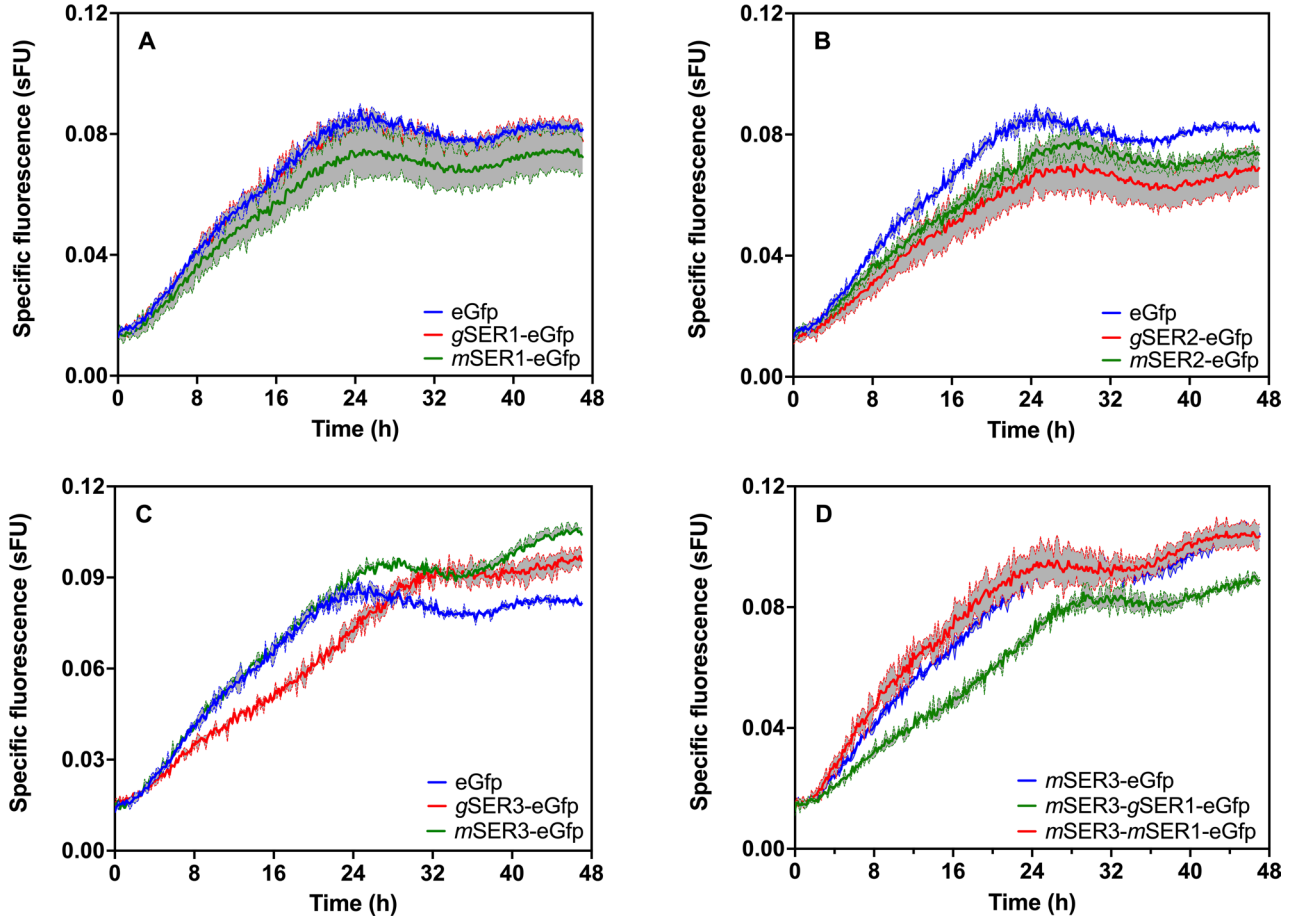

Fig. 2 Specific eGFP fluorescence for the eGfp strain (FdhKO P_{AOX1}-*eGFP*) expressing the *SER1* (**A**), *SER2* (**B**), *SER3* (**C**) and *SER1-SER3* (**D**) genes under the control of P_{GAP} (strains marked with *g*) and P_{MDH3} (strains marked with *m*) during growth in sorbitol medium (YNBS). The cells were grown in microbioreactors in batch mode as described in Materials and Methods. The specific fluorescence is the mean value (colored lines) and standard deviation (grey shading) of biological triplicates. sFU: specific fluorescence unit.

an order of magnitude lower than the concentration reported as cell toxic (20 mM [16]).

Enhancing serine metabolism in FdhKO strains increases the synthesis of secreted proteins

The FdhKO P_{MDH3}-*SER3* strain (hereafter *m*SER3) was further considered for its ability to produce a secretory protein, namely a glucose oxidase (Gox) from *Aspergillus niger*. Gox is an industrially relevant enzyme widely used in food processing, biosensing, and biocatalysis [32]. It is also a well-established model for secretory proteins [33–35]. The corresponding codon optimised sequence transcriptionally fused with the signal peptide from the α-mating factor from *S. cerevisiae* was cloned under the control of the P_{AOX1} promoter and expressed in FdhKO and *m*SER3 strains (Additional File1: Figure S3, Figure S4). As a first characterisation, the resulting GOX (fdh1Δ, P_{AOX1}-*αMF-GOX*) and GOX-*m*SER3 (fdh1Δ, P_{AOX1}-*αMF-GOX*, P_{MDH3}-*SER3*) strains were grown in shake flasks on sorbitol medium (YNBS) at medium OTC (Kla 50 h^{-1}) based on previous results [23]. Cell growth, Gox activity, formate and sorbitol concentration were measured at various time points for 72 h. At the end of cultivation, the GOX-*m*SER3 strain presented a 1.4-fold increase in Gox activity compared with that of the GOX strain, with respective values of 450 $U{\cdot}L^{-1}$ and 316 $U{\cdot}L^{-1}$ (Fig. 4A). Both strains exhibited similar growth kinetics, confirming that *SER3* overexpression does not impair cell fitness in those experimental conditions (Fig. 4C). As observed for the eGFP-expressing strains (Fig. 3), formate accumulated in both the GOX and GOX–*m*SER3 strains (Fig. 4B), with higher levels detected in the *SER3*-overexpressing strain. After 12 h of cultivation, formate concentrations reached 55 µM and 62 µM in the GOX and GOX–*m*SER3 strains, respectively. Subsequently, formate levels gradually decreased for both strains and became nearly undetectable after 72 h, despite continued cell growth and the presence of approximately 70% of the initial sorbitol in the culture medium (Fig. 4D). These results for secreted protein production are consistent

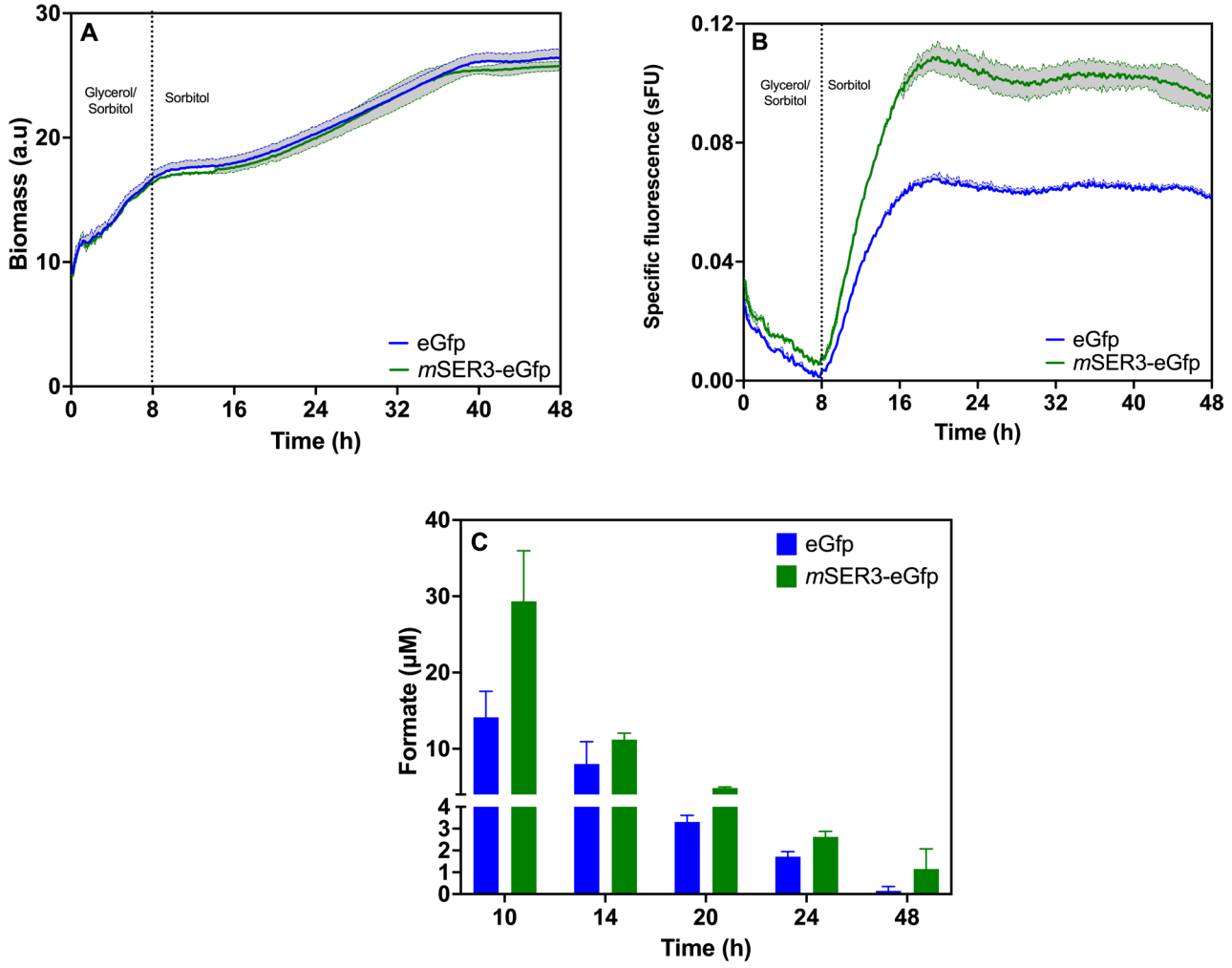

Fig. 3 Biomass (**A**), specific eGFP (**B**) and extracellular formate concentrations (**C**) for eGfp (fdh1Δ, P_{AOX1}-*eGFP*, blue color) and *m*SER3-eGfp (fdh1Δ, P_{AOX1}-*eGFP*, P_{MDH3}-*SER3*, green color) strains grown in YNB minimal media containing glycerol and sorbitol at a 1:2 ratio (YNBGS4). The cells were grown in microbioreactors in batch mode as described in "Materials and methods"s. The data represent the means and standard deviations of triplicate cultures. sFU: specific fluorescence unit; a.u: arbitrary units. μM: micromolar. In panels A and B, the vertical dotted line highlights the time point at which glycerol was depleted from the medium.

with the trends observed for the eGFP-expressing strains (i.e., eGfp and *m*SER3-eGfp strains, Fig. 3).

The GOX and GOX-*m*SER3 strains were further cultivated in batch mode in stirred-tank bioreactors with pH control using YNBGS medium containing glycerol and sorbitol at a 1:2 ratio. Biomass, GOX-specific activity, dissolved oxygen (DO) and carbon source concentrations were measured over 62-h. Culture conditions were set at 800 rpm agitation and 1 vvm aeration, corresponding to an experimentally determined k_La of 48 h^{-1} (data not shown).

Both strains exhibited diauxic growth, consuming glycerol during the first 15 h, followed by sorbitol over the subsequent 35 h (Fig. 5A, B). Glycerol depletion was indicated by a sharp increase in dissolved oxygen (DO) at 15 h (Fig. 5C). At this time point, glycerol was no longer detectable in the culture supernatant, whereas sorbitol consumption had not yet started (Fig. 5B). During the sorbitol consumption phase (i.e. between 25 h and 50 h), DO levels remained stable at approximately 85% air saturation, particularly for the GOX-mSER3 strain. Under these conditions, a pseudo-steady state with respect to DO can be assumed, such that the oxygen uptake rate (OUR) equals the oxygen transfer rate (OTR) [36]. This assumption allowed calculation of the cell-specific oxygen consumption rate (qO_2) by normalizing OTR values to the corresponding biomass. Based on biomass measurements obtained at multiple time points between 25 and 50 h of culture, the average qO_2 for the GOX-mSER3 strain was 3.4 mg $O_2 \cdot gDCW^{-1} \cdot h^{-1}$. Upon sorbitol depletion, DO increased to 100% saturation (Fig. 5C). Throughout the sorbitol consumption phase, both strains exhibited continuous growth with an average specific growth rate of 0.016 h^{-1} and a sorbitol uptake rate (qSor)

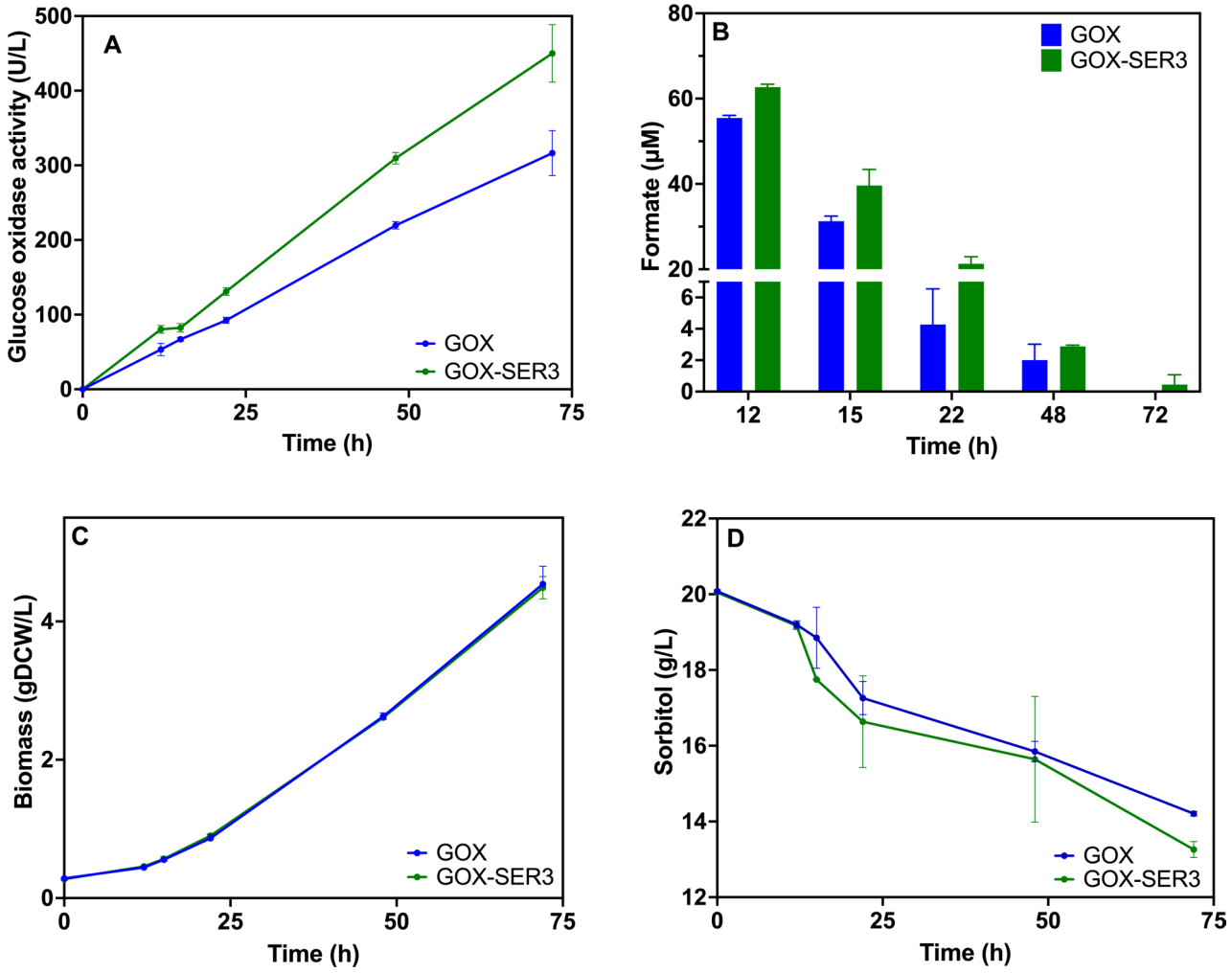

Fig. 4 Glucose oxidase activity (**A**), extracellular formate concentration (**B**), biomass (**C**) and sorbitol concentration (**D**) during the growth of the GOX (blue color) and GOX-*m*SER3 (green color) strains in sorbitol media (YNBS). The data are presented as the means and standard deviations of triplicate cultures conducted in shake flasks as described in Materials and Methods. Glucose oxidase assays were performed in triplicate, sorbitol and formate assays were performed in duplicate.

of 0.025 g·gDCW^{-1}·h^{-1}. Since oxygen was not limiting during rProt production on sorbitol, the calculated qO_2 and qSor values can be considered reference parameters for future process design. In particular, they can be used to estimate qO_2 at high cell densities (typically 60–100 gDCW·L^{-1}) and to define the operational conditions required to meet OTR demands and to establish appropriate sorbitol feeding strategies.

Most importantly, no Gox activity was detected in the culture supernatant during the glycerol consumption phase, confirming that the P_{AOX1} promoter is tightly repressed by glycerol. Upon glycerol depletion, Gox-specific activity increased almost linearly in both strains, reaching a plateau after 40 h. At the end of the culture, the Gox-specific activity of the GOX-*m*SER3 strain was 1.3-fold higher than that of the GOX strain (Fig. 5D). The enzymatic productivities calculated over a 47-h production period were 0.31 and 0.39 U·gDCW^{-1}·h^{-1} for strains GOX and GOX-*m*SER3, respectively.

These observations have important implications for future process development. In most processes, rProt production is temporally separated from biomass formation. Typically, cells are first grown in batch or fed-batch under conditions that repress P_{AOX1}, with glycerol as the primary carbon source. The rProt production phase is then initiated by shifting to permissive culture conditions, most commonly through methanol supplementation. The main technical challenge lies in determining the optimal timing and methodology for transitioning from repressive to inducible conditions. In addition, cells must adapt to methanol, a process that requires extensive metabolic reorganization. Formate has been proposed and successfully tested, in combination with an FdhKO strain, as an alternative inducer to methanol [21]. Using CalB as

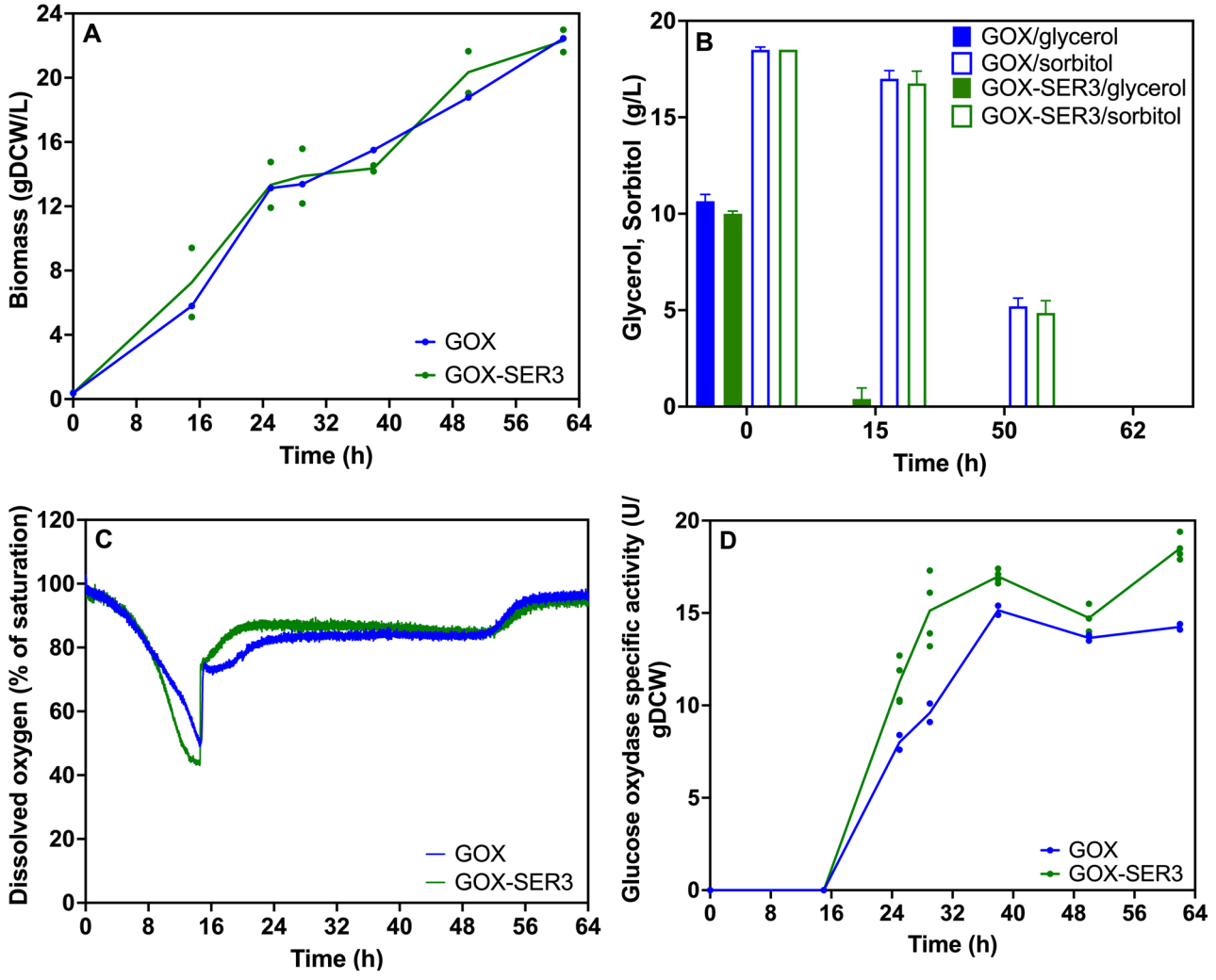

Fig. 5 Biomass (**A**), glycerol (filled histograms) and sorbitol (empty histograms) concentrations (**B**), dissolved oxygen (**C**), and glucose oxidase-specific activity (**D**) during the growth of the GOX (blue colour) and GOX-SER3 (green colour) strains in a stirred-tank bioreactor in batch mode as described in Materials and Methods in glycerol-sorbitol media (YNBGS). Cultures were performed in duplicate. In **A** and **D**, the dots represent all the measurements, while the lines connect the mean values

a model secreted protein, a maximum specific activity of 136 U·mgDCW^{-1} was achieved on sorbitol with a FdhKO CalB strain, compared to 113 U·mgDCW^{-1} obtained with a Fdh CalB strain using methanol as the inducer. In addition, this maximum specific activity was reached 2.4-fold faster with the FdhKO CalB strain on sorbitol medium.

Therefore, the limitations associated with methanol-based induction can be overcome by cultivating FdhKO strains in media containing both glycerol and sorbitol, with the glycerol supply adjusted to reach the desired biomass. Upon glycerol depletion, P_{AOX1} repression is relived, and sorbitol becomes the primary carbon and energy source. In contrast to methanol, sorbitol catabolism requires only minor metabolic adaptation. Under these conditions, formate generated via THF-C1 pathway accumulates intracellularly in FdhKO strains, inducing P_{AOX1} and initiating the rProt production phase. In such a way, no external inducer is requested as the P_{AOX1} is auto-induced by endogenous formate. Overexpression of *SER3* further enhance this autoinduction effect. Importantly, compared to methanol-based processes, optimal culture performance can be achieved at lower OTR, a highly advantageous feature for large-scale bioprocess development, where oxygen transfer is often a key limitation. Consistently, the qO_2 values determined in this study for sorbitol (≈ 4 mgO_2·gDCW^{-1}·h^{-1}) are substantially lower than those reported for methanol-based processes (120–170 mgO_2·gDCW^{-1}·h^{-1}; [19, 37]).

Conclusions

In *K. phaffii*, *AOX1* promoter–based expression systems have proven highly effective for rProt production. However, the use of methanol at industrial scale is associated with several challenges that increase process

complexity and cost. Consequently, methanol-free induction strategies have been actively explored. These include the use of derepressed promoters, such as the recently reported P_{DH}, which is induced under the so-called pseudo-starvation conditions [13, 14], as well as the use of alternative inducers for P_{AOX1}, notably formate [16]. Nevertheless, due to the low energy content of formate, its use as an inducer requires the presence of a permissive carbon source, such as sorbitol. In addition, formate-based induction presents further challenges, as formate becomes toxic to cells at concentrations above approximately 20 mM [16].

Recently, we reported that disruption of the formate dehydrogenase gene in *K. phaffii* leads to formate accumulation when FdhKO cells are grown on sorbitol, but not on glycerol. This enables *AOX1* promoter–based expression systems to operate in a self-inducible manner, thereby eliminating the need for methanol as an external inducer and its associated issues. Specifically, for FdhKO cells cultivated in a glycerol–sorbitol mixture, P_{AOX1} induction is triggered only after glycerol depletion. The low growth rate of the FdhKO strain on sorbitol favors the accumulation of endogenous formate required for P_{AOX1} activation, while sorbitol provides the necessary energy supply for rProt synthesis.

In the present study, we aimed to further enhance endogenous formate accumulation by engineering serine metabolism. Overexpression of the gene encoding 3-phosphoglycerate dehydrogenase in a formate dehydrogenase-deficient *K. phaffii* strain significantly increased formate accumulation without compromising cell fitness and markedly enhanced P_{AOX1} induction under derepressed culture conditions. This strategy further improved rProt productivity, as exemplified by a 30% increase in Gox secretion under bioreactor process conditions.

Materials and methods

Strains construction

The *Escherichia coli* and *K. phaffii* strains used in this study are listed in Table 1 and supporting information Table S2. The general genetic techniques used were previously described [21]. The plasmids, GoldenPiCS genetic parts and primers used are listed in the Additional File 1: Tables S2 and S3. The DNA sequence of the signal peptide of the alpha mating factor (*α*MF) from *Saccharomyces cerevisiae* (NM_001184001.1) and the intron-less coding sequence of the glucose oxidase (Gox) gene from *A. niger* (x60601.1) were codon optimized for *K. phaffii* using SnapGene software (GSL Biotech LLC, Boston, MA). Codons with a frequency less than 10% were replaced with the most abundant coding for the same amino acid. The recognition sequences for *Bsa*I or *Bpi*I were added to the coding sequences as shown in Additional File 1: Figures S3 and S4. The *α*MF and Gox synthetic DNA fragments obtained from IDT technologies (Leuven Belgium) were subsequently cloned and inserted into the pUC57 and pGEM-T Easy vectors, respectively, to yield the plasmids RIE457 and RIE585 (Supporting Information Table S1). The *α*MF plasmid (RIE457) was digested by *Bsa*I and ligated at the corresponding site of plasmid A2 (BB1_23), yielding the plasmid RIE504 (A2_BB1_23_*αMFGOX*). The plasmid RIE507 (BB3aZ_14-P_{AOX1}-*αMF-GOX-SsCy1*tt) was obtained by GoldenGate assembly from plasmids B8 (BB1_12_P_{AOX1}), C1 (BB1_34_*ScCYC1*tt), D12 (BB3aZ_14) and RIE504, using *Bpi*I as the restriction enzyme as described elsewhere [29]. The correctness of the assembly was verified by DNA sequencing using the primer pair CkBB3aZ14-Fw/CkBB3aZ1-Rv.

The genes PAS_chr3_0566 (*SER1*), PAS_chr4_0285 (*SER2*), and PAS_chr2-1_0657 (*SER3*) were PCR-amplified from *K. Phaffii* GS115pro genomic DNA used as a template using the primer pairs SER1-Fw/SER1-Rv, SER2-Fw/SER2-Rv and SER3-Fw/SER3-Rv, respectively. The resulting PCR fragments were subsequently inserted into the ZeroBlunt TOPO vector, yielding the plasmids RIE508 (TOPO_*SER1*), RIE509 (TOPO_*SER2*), and RIE510 (TOPO_*SER3*), respectively. Positive constructs were verified by DNA sequencing with M13-Fw/M13-Rv primers. To construct the SER gene expression vectors, the promoter, gene and terminator parts were first PCR amplified using the specific primer pairs designed to generate specific overlaps for subsequent Gibson assembly using the NEBuilder Hifi DNA Assembly Kit (New England Biolabs). The P_{GAP} fragments were PCR amplified from plasmid A4 (BB1_12_P_{GAP}) using the primer pairs 1.pGAP.SER1-Rv/2.pGAP-Fw; 1.pGAP.SER2-Rv/2.pGAP-Fw; and 1.pGAP.SER3-Rv/2.pGAP-Fw to generate parts 1, 2 and 3, respectively. The P_{MDH3} fragments were PCR amplified from plasmid A9 (BB1_12_P_{MDH3}) using the primer pairs 1.pMDH3.SER1-Rv/2.pMDH3-Fw; 1.pMDH3.SER2-Rv/2.pMDH3-Fw, 1.pMDH3.SER3-Rv/2.pMDH3-Fw and 1.pMDH3.SER3-Rv/1. BB3rN14pMDH3-Fw to generate parts 4, 5, 6 and 7, respectively. *SER1* gene fragments were amplified from the RIE508 plasmid (TOPO_*SER1*) using the primer pairs 3.SER1Rv/2.pGAP. SER1Fw and 3.SER1Rv/2.pMDH3.SER1Fw to generate parts 8 and 9, respectively. The *SER2* gene fragment was amplified from the RIE509 plasmid (TOPO_*SER2*) using the primer pairs 3.SER2Rv/2.pGAP. SER2Fw and 3.SER2Rv/2.pMDH3.SER2Fw to generate parts 10 and 11, respectively. *SER3* gene fragments were amplified from the RIE510 plasmid (TOPO_*SER3*) using the primer pairs 3.SER3Rv/2.pGAP. SER3Fw and 3.SER3Rv/2.pMDH3. SER3Fw to generate parts 12 and 13, respectively. The *ScCYC1* terminator fragments were PCR amplified from plasmid C1 (BB1_34_*ScCYC1*tt) using the primer pairs

4.CYC1-Rv/4.SER1. C1-Fw; 4.BB3eH14.C1-Rv/4.SER1. C1-Fw, 4.CYC1-Rv/4.SER2.C1-Fw; 4.CYC1-Rv/4.SER3. C1-Fw and 4.BB3rN14.C1-Rv/4.SER3.C1-Fw to generate parts 14, 15, 16, 17 and 18, respectively. All the obtained PCR fragments were gel purified and quantified with a NanoDrop system (Thermo Fisher Scientific). The final expression vectors were obtained by Gibson assembly as follows: parts 1, 8, 14 and D12 plasmid *Bpi*I digested to obtain plasmid RIP511 (BB3aZ_14-P_{GAP}-*SER1-SsCy1*tt); parts 4, 9, 14 and D12 plasmid *Bpi*I digested to obtain plasmid RIP512 (BB3aZ_14-P_{MDH3}-*SER1-SsCy1*tt); parts 2, 10, 16 and D12 plasmid *Bpi*I digested to obtain plasmid RIP513 (BB3aZ_14-P_{GAP}-*SER2-SsCy1*tt); parts 5, 11, 16 and D12 plasmid *Bpi*I digested to obtain plasmid RIP514 (BB3aZ_14-P_{MDH3}-*SER2-SsCy1*tt); parts 1, 12, 17 and D12 plasmid *Bpi*I digested to obtain plasmid RIP515 (BB3aZ_14-P_{GAP}-*SER3-ScCYC1*tt); parts 6, 13, 17 and D12 plasmid *Bpi*I digested to obtain plasmid RIP516 (BB3aZ_14-P_{MDH3}-*SER3-ScCYC1*tt). The correctness of the assembly constructs was verified by PCR with the primer pair CkBB3aZ14-Fw/CkBB3aZ1-Rv for RIP511, RIP512, RIP513, RIP, RIP514, RIP515 and RIP516; 1BB3aZ14-Rv/4. BB3eH14-Fw for RIP517, RIP518 and 1.BB3rN14-Rv/4. BB3rN14-Fw for RIP519. The correctness of the plasmid sequence was verified by DNA sequencing.

The construction of the yeast strains RIY230 (Fdh eGfp), RIY536 (FdhKO eGfp Z^+), and RIY540 (eGfp) is described elsewhere [21]. Strains RIY657 *(*fdh1Δ, P_{GAP}-*SER1*, P_{AOX1}-*eGFP*, hereafter *g*SER1-eGfp), RIY658 (fdh1Δ, P_{MDH3}-*SER1*, P_{AOX1}-*eGFP*, hereafter *m*SER1-eGfp), RIY659 (fdh1Δ, P_{GAP}-*SER2*, P_{AOX1}-*eGFP*, hereafter *g*SER2-eGfp), RIY660 (fdh1Δ, P_{MDH3}-*SER2*, P_{AOX1}-*eGFP*, hereafter *m*SER2-eGfp strain), RIY661 (fdh1Δ, P_{GAP}-*SER3*, P_{AOX1}-*eGFP*, hereafter *g*SER3-eGfp), and RIY662 (fdh1Δ, P_{MDH3}-*SER3*, P_{AOX1}-*eGFP*, hereafter *m*SER3-eGfp strain) were obtained via the transformation of strain RIY540 with *Asc*I linearized plasmids RIP511, RIP512, RIP513, RIP514, RIP515, and RIP516, respectively, which target integration at the *AOX1*tt locus. Strains RIY663 (fdh1Δ, P_{MDH3}-*SER3*, P_{GAP}-*SER1*, P_{AOX1}-*eGFP*, hereafter referred to as the *m*SER3-*g*SER1-eGfp strain) and RIY664 (fdh1Δ, P_{MDH3}-*SER3*, P_{MDH3}-*SER1*, P_{AOX1}-*eGFP*, *m*SER3-*m*SER1-eGfp) were obtained by transformation of strain RIY662 with *Pme*I linearized plasmids RIP517 and RIP518, respectively, to target the integration at the *ENO1* locus.

For marker rescue, the RIY538 (FdhKO Z^+) strain was transformed with the replicative vector RIP396 (pKTAC-Cre), and transformants were selected on YPD-Genet. The resulting strain was RIY539 (FdhKO). The RIY655 (fdh1Δ, P_{AOX1}-*αMF-GOX*, hereafter referred to as GOX) strain was obtained by the transformation of strain RIY539 with *Asc*I linearized plasmid RIP507 for the integration of the expression cassette at the *AOX1*tt locus. The RIY665 strain (fdh1Δ, P_{AOX1}-*αMF-GOX*, P_{MDH3}-*SER3*, hereafter the SER3-GOX strain) was obtained by the transformation of strain RIY655 with *Asc*I linearized plasmid RIP519 for the integration of the expression cassette at the *RIG2* locus. The genotypes of the RIY655, RIY657, RIY658, RIY659, RIY660, RIY661 and RIY662 strains were verified by PCR using the primers CkBB3aZ14-Fw/CkBB3aZ1-Rv, whereas those of the RIY663 and RIY664 strains were verified using the primers 1BB3aZ14-Rv/4.BB3eH14-Fw. The genotype of the RIY665 strain was verified by PCR using the primers 1.BB3rN14-Rv/4.BB3rN14-Fw. Each primer pair was annealed to the 5´ and 3´ regions of the integrated construct. A schematic representation of the strain genotype is presented in Additional File 1: Figure S5. Monocopy integration of the SER and GOX gene expression cassettes in the yeast genome was assessed for the different constructed strains (Additional File 1: Figures S5 and S6).

Medium composition

YPD media contained 20 $g{\cdot}L^{-1}$ glucose, 10 $g{\cdot}L^{-1}$ Difco yeast extract, and 10 $g{\cdot}L^{-1}$ Difco bacto peptone. YNB media contained 1.7 $g{\cdot}L^{-1}$ Difco YNB w/o ammonium chloride and amino acids, 5 $g{\cdot}L^{-1}$ NH_4Cl, 0.4 $mg{\cdot}L^{-1}$ biotin and carbon source as follows: 1.75 $g{\cdot}L^{-1}$ glycerol and 3.5 $g{\cdot}L^{-1}$ sorbitol (YNBGS4), 20 $g{\cdot}L^{-1}$ sorbitol (YNBS) or 20 $g{\cdot}L^{-1}$ glycerol and 20 $g{\cdot}L^{-1}$ sorbitol (YNBGS). All media contained 100 mM sodium/potassium phosphate buffer, pH 6.0.

Cultures conditions

All *K. phaffii* cultures were performed at 30 °C. Precultures were performed as previously described [21]. Shake flask cultures were performed in 250 ml Erlenmeyer flasks containing 25 ml of YNBS with agitation at 150 rpm. Cultures in microbioreactors (BioLector 2, m2p-labs, Baesweiler, Germany) were operated in batch mode without pH and DO control at 1000 rpm with a relative humidity of 85% using 48-well flower plates (M2P-MTP-48B, Beckman Coulter) containing 1 ml of YNBS or YNBGS4 medium.

Stirred tank bioreactor cultivations were performed in 155 ml of YNBGS medium in 200-ml DASGIP bioreactors (DASGIP DASbox Mini Bioreactors SR0250ODLS, Eppendorf, Hamburg, Germany) at 30 °C as described previously [30]. The operating parameters were as follows: aeration at 0.5 vvm, stirring at 900 rpm and the pH automatically controlled at 6 by the addition of 3 N KOH.

Calculations

The specific growth rate was calculated as

$$\mu = \frac{1}{X}\frac{dX}{dt}$$

where X is the biomass (gDCW·L^{-1}) and t is the time (h).

The specific sorbitol up-take rate was calculated as

$$qSor = \frac{d\,[sorbitol]}{dX.t}$$

where [sorbitol] is the sorbitol concentration, X the biomass (gDCW·L^{-1}) and t is the time (h).

The oxygen transfer rate was calculated as

$$OTR = k_L a(C_0 - C_L)$$

Where $k_L a$ is the volumetric oxygen transfer coefficient determined using the dynamic method of desroption-absorpion of oxygen [38], C_0 is the oxygen concentration at equilibrium, which according to Henry's law equals 7.6 mg·L^{-1} [19] and C_L is the measured dissolved oxygen concentration (DO·C_0, mg L^{-1}).

The specific oxygen consumption rate (qO_2) was calculated as

$$qO2 = \frac{OTR}{dX} = \frac{k_L a(C_0 - C_L)}{X}$$

Where C_0 is the oxygen concentration at equilibrium, C_L is the measured dissolved oxygen concentration (mg·L^{-1}) and X is the biomass (gDCW·L^{-1}).

Analytical methods

The cell growth was monitored either by optical density at 600 nm (OD600) or dry cell weight (DCW) as previously described [31]. Sorbitol and glycerol concentrations were determined by high-performance liquid chromatography (Agilent 1100 series equipped with a UV (210 nm) and RID detector (Agilent Technologies, Santa Clara, CA, USA) and an Aminex HPX-87 H column (300 × 7.8 mm; Bio-Rad, Hercules, CA, USA). The compounds were eluted from the column at 65 °C at a flow rate of 0.5 mL·min^{-1}, and a 5 mM H_2SO_4 solution was used as the mobile phase. During culture in microbioreactors, biomass was monitored by light scattering at 600 nm (gain set at 2), whereas fluorescence was quantified at 520 nm (excitation 488 nm, gain set at 4) every 10 min. eGFP fluorescence was expressed as specific fluorescence (sFU). For that purpose, the fluorescence values were divided by the biomass values. The specific fluorescence value of the parental strain GS115pro (RIY232) was subtracted from the specific fluorescence of the eGFP-producing strains to normalize the data.

The formate concentration in the culture supernatant was measured using the formic acid assay kit (Megazyme Inc., Bray, Ireland) according to the manufacturer's instructions. Briefly, formate is converted into carbon dioxide by formate dehydrogenase with the formation of NADPH, which is quantified at 340 nm. The formate concentration is deduced from a calibration curve.

Glucose oxidase activity was monitored using a glucose oxidase assay kit (Megazyme Inc., Bray, Ireland) according to the manufacturer's instructions. Briefly, Gox catalyzes the oxidation of β-D-glucose to D-glucono-δ-lactone with the concurrent release of hydrogen peroxide. In the presence of peroxidase, the H_2O_2 generated is converted, in the presence of p-hydroxybenzoic acid, into quinoneimine, which is measured at 510 nm. Gox activity was calculated based on a standard curve. For the formate and enzymatic assays, absorbances at specific wavelengths were monitored over time using a SpectraMax M2 (Molecular Devices, San Jose, CA, USA). All the assays were conducted in triplicate.

Supplementary Information

The online version contains supplementary material available at https://doi.org/10.1186/s12934-026-02968-1.

Supplementary Material 1

Acknowledgements

The authors wish to thank Samuel Telek for his help with the bioreactor culture and Cristina Bustos for sharing some of the strains used in this study.

Author contributions

PF and RC design the experiments and analyse the results. RC performed the experiments and prepared the draft of the manuscript. PF and JB secure the fundings. All the authors contributed to editing the draft and approved the final manuscript.

Funding

ERASMUS + 2022–2023 Grant agreement for mobility participants - Higher education (PIC:999854952, E10208749); Wallonie-Bruxelles International, Cooperation bilateral Belgique-Chili project SUB/2019/435787 (RIO4), SUB/2023/591923/MOD (RI06) and SUB/2023/585456 (RC06). R. Cozmar was funded by Beca Doctorado Nacional grant number 21211350-Agencia Nacional de Investigación y Desarrollo (ANID), Chile; Doctoral Internship Scholarship (PUCV, Chile).

Data availability

No datasets were generated or analysed during the current study.

Declarations

Ethics approval and consent to participate

Not applicable.

Consent for publication

Not applicable.

Competing interests

The authors declare no competing interests.

Received: 10 November 2025 / Accepted: 18 February 2026
Published online: 08 March 2026

References

1. Heistinger L, Gasser B, Mattanovich D. Microbe profile: *Komagataella phaffii*: a methanol devouring biotech yeast formerly known as *Pichia pastoris*. Microbiology. 2020;166(7):614–6. https://doi.org/10.1099/mic.0.000958.
2. Barone GD, Emmerstorfer-Augustin A, Biundo A, Pisano I, Coccetti P, Mapelli V, et al. Industrial production of proteins with *Pichia pastoris-Komagataella phaffii*. Biomolecules. 2023;13(3):441. https://doi.org/10.3390/biom13030441.
3. Vogl T, Glieder A. Regulation of *Pichia pastoris* promoters and its consequences for protein production. N Biotechnol. 2013;30(4):385–404. https://doi.org/10.1016/j.nbt.2012.11.010.
4. Liang S, Zou C, Lin Y, Zhang X, Ye Y. Identification and characterization of PGCW14: a novel, strong constitutive promoter of *Pichia pastoris*. Biotechnol Lett. 2013;35(11):1865–71. https://doi.org/10.1007/s10529-013-1265-8.
5. Hartner FS, Glieder A. Regulation of methanol utilisation pathway genes in yeasts. Microb Cell Fact. 2006;5(1):39. https://doi.org/10.1186/1475-2859-5-39.
6. Potvin G, Ahmad A, Zhang Z. Bioprocess engineering aspects of heterologous protein production in *Pichia pastoris*: a review. Biochem Eng J. 2012;64:91–105. https://doi.org/10.1016/j.bej.2010.07.017.
7. Cereghino JL, Cregg JM. Heterologous protein expression in the methylotrophic yeast *Pichia pastoris*. FEMS Microbiol Rev. 2000;24(1):45–66. https://doi.org/10.1111/j.1574-6976.2000.tb00532.x.
8. Hartner FS, Ruth C, Langenegger D, Johnson SN, Hyka P, Lin-Cereghino GP, et al. Promoter library designed for fine-tuned gene expression in *Pichia pastoris*. Nucleic Acids Res. 2008;36(12):e76. https://doi.org/10.1093/nar/gkn369.
9. Niu H, Jost L, Pirlot N, Sassi H, Daukandt M, Rodriguez C, et al. A quantitative study of methanol/sorbitol co-feeding process of a *Pichia pastoris* Mut+/*pAOX1*-lacZ strain. Microb Cell Fact. 2013;12(1):33. https://doi.org/10.1186/1475-2859-12-33.
10. Çelik E, Çalık P, Oliver SG. Fed-batch methanol feeding strategy for recombinant protein production by *Pichia pastoris* in the presence of co-substrate sorbitol. Yeast. 2009;26(9):473–84. https://doi.org/10.1002/yea.1679.
11. Ergün BG, Berrios J, Binay B, Fickers P. Recombinant protein production in *Pichia pastoris*: from transcriptionally redesigned strains to bioprocess optimization and metabolic modelling. FEMS Yeast Res. 2021;21(7):foab057. https://doi.org/10.1093/femsyr/foab057.
12. Bustos C, Quezada J, Veas R, Altamirano C, Braun-Galleani S, Fickers P, et al. Advances in cell engineering of the *Komagataella phaffii* platform for recombinant protein production. Metabolites. 2022;12(4):346. https://doi.org/10.3390/metabo12040346.
13. Bernat-Camps N, Ebner K, Schusterbauer V, Fischer JE, Nieto-Taype MA, Valero F, et al. Enabling growth-decoupled *Komagataella phaffii* recombinant protein production based on the methanol-free PDH promoter. Front Bioeng Biotechnol. 2023;1130583. https://doi.org/10.3389/fbioe.2023.1130583.
14. Ebner K, Bernat-Camps N, Scheipel S, Dörner C, Valero F, Glieder A, et al. Next-generation stress-inducible *Komagataella phaffii* promoter variants. Microb Cell Fact. 2025;24(1):228. https://doi.org/10.1186/s12934-025-02825-7.
15. Jayachandran C, Palanisamy Athiyaman B, Sankaranarayanan M. Formate co-feeding improved Candida antarctica Lipase B activity in *Pichia pastoris*. Res J Biotechnol. 2017;12(12):29–36.
16. Singh A, Narang A. The Mut+ strain of *Komagataella phaffii* (*Pichia pastoris*) expresses *PAOX1* 5 and 10 times faster than Muts and Mut– strains: evidence that formaldehyde or/and formate are true inducers of *PAOX1*. Appl Microbiol Biotechnol. 2020;104(18):7801–14. https://doi.org/10.1007/s00253-020-10793-8.
17. Tyurin OV, Kozlov DG. Deletion of the FLD gene in methylotrophic yeasts *Komagataella phaffii* and *Komagataella kurtzmanii* results in enhanced induction of the *AOX1* promoter in response to either methanol or formate. Microbiol (N Y). 2015;84(3):408–11. https://doi.org/10.1134/S0026261715030212.
18. Liu B, Zhao Y, Zhou H, Zhang J. Enhancing xylanase expression of *Komagataella phaffii* induced by formate through Mit1 co-expression. Bioprocess Biosyst Eng. 2022;45(9):1515–25. https://doi.org/10.1007/s00449-022-02760-6.
19. Berrios J, Flores MO, Díaz-Barrera A, Altamirano C, Martínez I, Cabrera Z. A comparative study of glycerol and sorbitol as co-substrates in methanol-induced cultures of *Pichia pastoris* : temperature effect and scale-up simulation. J Ind Microbiol Biotechnol. 2017;44(3):407–11. https://doi.org/10.1007/s10295-016-1895-7.
20. Christensen KE, MacKenzie RE. Mitochondrial one-carbon metabolism is adapted to the specific needs of yeast, plants and mammals. Bioessays. 2006;28(6):595–605. https://doi.org/10.1002/bies.20420.
21. Bustos C, Berrios J, Fickers P. Formate from THF-C1 metabolism induces the *AOX1* promoter in formate dehydrogenase-deficient *Komagataella phaffii*. Microb Biotechnol. 2024;17(10):e70022. https://doi.org/10.1111/1751-7915.70022.
22. Casal M, Paiva S, Queirós O, Soares-Silva I. Transport of carboxylic acids in yeasts. FEMS Microbiol Rev. 2008;32(6):974–94. https://doi.org/10.1111/j.1574-6976.2008.00128.x.
23. Bustos C, Cozmar R, Berrios J, Fickers P. Sorbitol uptake and oxygen transfer shape *AOX1* promoter induction in formate dehydrogenase-deficient *Komagataella phaffii*. Microb Biotechnol. 2025;18(11):e70263. https://doi.org/10.1111/1751-7915.70263.
24. Pruneski JA, Hainer SJ, Petrov KO, Martens JA. The Paf1 complex represses *SER3* transcription in Saccharomyces cerevisiae by facilitating intergenic transcription-dependent nucleosome occupancy of the *SER3* promoter. Eukaryot Cell. 2011;10(10):1283–94. https://doi.org/10.1128/EC.05141-11.
25. Kobayashi J, Sasaki D, Hara KY, Hasunuma T, Kondo A. Metabolic engineering of the l-serine biosynthetic pathway improves glutathione production in *Saccharomyces cerevisiae*. Microb Cell Fact. 2022;21(1):153. https://doi.org/10.1186/s12934-022-01880-8.
26. Delic M, Mattanovich D, Gasser B. Repressible promoters – a novel tool to generate conditional mutants in *Pichia pastoris*. Microb Cell Fact. 2013;12(1):6. https://doi.org/10.1186/1475-2859-12-6.
27. Martens JA, Wu PYJ, Winston F. Regulation of an intergenic transcript controls adjacent gene transcription in *Saccharomyces cerevisiae*. Genes Dev. 2005;19(22):2695–704. https://doi.org/10.1101/gad.1367605.
28. Esch BM, Limar S, Bogdanowski A, Gournas C, More T, Sundag C, et al. Uptake of exogenous serine is important to maintain sphingolipid homeostasis in *Saccharomyces cerevisiae*. PLoS Genet. 2020;16(8):e1008745. https://doi.org/10.1371/journal.pgen.1008745.
29. Prielhofer R, Barrero JJ, Steuer S, Gassler T, Zahrl R, Baumann K, et al. GoldenPiCS: a golden gate-derived modular cloning system for applied synthetic biology in the yeast *Pichia pastoris*. BMC Syst Biol. 2017;11(1):123. https://doi.org/10.1186/s12918-017-0492-3.
30. Theron CW, Berrios J, Steels S, Telek S, Lecler R, Rodriguez C, et al. Expression of recombinant enhanced green fluorescent protein provides insight into foreign gene-expression differences between Mut + and MutS strains of *Pichia pastoris*. Yeast. 2019;36(5):285–96. https://doi.org/10.1002/yea.3388.
31. Carly F, Niu H, Delvigne F, Fickers P. Influence of methanol/sorbitol co-feeding rate on *pAOX1* induction in a *Pichia pastoris* Mut+ strain in bioreactor with limited oxygen transfer rate. J Ind Microbiol Biotechnol. 2016;43(4):517–23. https://doi.org/10.1007/s10295-015-1722-6.
32. Bankar SB, Bule MV, Singhal RS, Ananthanarayan L. Glucose oxidase — an overview. Biotechnol Adv. 2009;27(4):489–501. https://doi.org/10.1016/j.biotechadv.2009.04.003.
33. Çelik E, Çalık P. Production of recombinant proteins by yeast cells. Biotechnol Adv. 2012;30(5):1108–18. https://doi.org/10.1016/j.biotechadv.2011.09.011.
34. Ahmad M, Hirz M, Pichler H, Schwab H. Protein expression in *Pichia pastoris*: recent achievements and perspectives for heterologous protein production. Appl Microbiol Biotechnol. 2014;98(12):5301–17. https://doi.org/10.1007/s00253-014-5732-5.
35. Yu S, Miao L, Huang H, Li Y, Zhu T. High-level production of glucose oxidase in *Pichia pastoris*: effects of Hac1p overexpression on cell physiology and enzyme expression. Enzyme Microb Technol. 2020;141:109671. https://doi.org/10.1016/j.enzmictec.2020.109671.
36. Liang J, Yuan J. Oxygen transfer model in recombinant *Pichia pastoris* and its application in biomass estimation. Biotechnol Lett. 2007;29(1):27–35. https://doi.org/10.1007/s10529-006-9203-7.
37. Velastegui E, Quezada J, Altamirano C, Berrios J, Fickers P. Co-feeding strategy alleviates hypoxic stress in large-scale bioreactor for optimal production of secretory recombinant proteins in *Pichia pastoris*. J Biotechnol. 2023;373:20–3. https://doi.org/10.1016/j.jbiotec.2023.06.006.
38. Garcia-Ochoa F, Gomez E. Bioreactor scale-up and oxygen transfer rate in microbial processes: an overview. Biotechnol Adv. 2009;27:153–76. https://doi.org/10.1016/j.biotechadv.2008.10.006.

Publisher's Note